

# Automated mapping of *Portulacaria afra* canopies for restoration monitoring with convolutional neural networks and heterogeneous unmanned aerial vehicle imagery

Nicholas C Galuszynski<sup>Equal first author, 1</sup>, Robbert Duker<sup>Equal first author, 1</sup>, Alastair J. Potts<sup>Corresp., 1</sup>, Teja Kattenborn<sup>2, 3</sup>

<sup>1</sup> Department of Botany, Nelson Mandela University, Gqeberha, South Africa

<sup>2</sup> Remote Sensing Centre for Earth System Research (RSC4Earth), Universität Leipzig, Leipzig, Germany

<sup>3</sup> German Centre for Integrative Biodiversity Research (iDiv), Halle-Jena-Leipzig, Leipzig, Germany

Corresponding Author: Alastair J. Potts

Email address: alastair.potts@mandela.ac.za

Ecosystem restoration and reforestation initiatives can operate at large spatial scales, whereas monitoring is often limited to spatially restricted field measures that are time- and -labour intensive and unable to accurately cover the hundreds to thousands of hectares under restoration. Recent advances in remote sensing technologies coupled with deep learning algorithms provide an unprecedented opportunity for monitoring changes in vegetation cover at spatial and temporal scales. Data generated in this manner can feed directly into adaptive management practices and provide insights into regeneration dynamics. Here we demonstrate that coupling imagery acquired using different models of Unoccupied Aerial Vehicles (UAVs), and under heterogeneous illumination conditions, with Convolutional Neural Network (CNN) segmentation algorithms accurately classified the canopy cover of *Portulacaria afra* Jacq. - the target species for the restoration of Albany Subtropical Thicket vegetation, endemic to South Africa. The model presented here is widely transferable to restoration monitoring as its application does not require any knowledge of the CNN model, or specialist training, can be applied to imagery generated by a range of UAV models, and will reduce the sampling effort required to track restoration trajectories in space and time. This will contribute to more effective management or restoration sites and promote collaboration between scientists and practitioners.

# 1 Automated mapping of *Portulacaria afra* canopies for 2 restoration monitoring with convolutional neural 3 networks and heterogeneous Unmanned Aerial 4 Vehicle imagery

5

6 Nicholas C Galuszynski <sup>Equal first author, 1</sup>, Robbert Duker <sup>Equal first author, 1</sup>, Alastair J. Potts <sup>Corresp., 1</sup>,  
7 Teja Kattenborn <sup>2, 3</sup>

8

9 <sup>1</sup>Department of Botany, Nelson Mandela University, Gqeberha, South Africa

10 <sup>2</sup>Remote Sensing Centre for Earth System Research (RSC4Earth), Universität Leipzig, Leipzig, Germany

11 <sup>3</sup>German Centre for Integrative Biodiversity Research (iDiv), Halle-Jena-Leipzig, Leipzig, Germany

12

13 Corresponding Author: Alastair J. Potts

14 Email address: [alastair.potts@mandela.ac.za](mailto:alastair.potts@mandela.ac.za)

15

## 16 Abstract

17 Ecosystem restoration and reforestation initiatives can operate at large spatial scales, whereas  
18 monitoring is often limited to spatially restricted field measures that are time- and -labour  
19 intensive and unable to accurately cover the hundreds to thousands of hectares under  
20 restoration. Recent advances in remote sensing technologies coupled with deep learning  
21 algorithms provide an unprecedented opportunity for monitoring changes in vegetation cover at  
22 spatial and temporal scales. Data generated in this manner can feed directly into adaptive  
23 management practices and provide insights into regeneration dynamics. Here we demonstrate  
24 that coupling imagery acquired using different models of Unoccupied Aerial Vehicles (UAVs),  
25 and under heterogeneous illumination conditions, with Convolutional Neural Network (CNN)  
26 segmentation algorithms accurately classified the canopy cover of *Portulacaria afra* Jacq. - the  
27 target species for the restoration of Albany Subtropical Thicket vegetation, endemic to South  
28 Africa. The model presented here is widely transferable to restoration monitoring as its  
29 application does not require any knowledge of the CNN model or specialist training, can be  
30 applied to imagery generated by a range of UAV models, and will reduce the sampling effort  
31 required to track restoration trajectories in space and time. This will contribute to more effective  
32 management or restoration sites and promote collaboration between scientists and  
33 practitioners.

## 34 Introduction

35 With the United Nations “Decade on Ecosystem Restoration” underway, there are likely to be  
36 global increases in the extent of restoration initiatives. These initiatives will require methods for  
37 accurately monitoring the trajectories of restoration efforts in an efficient and cost-effective  
38 manner (de Almeida et al., 2020; Méndez-Toribio et al., 2021; Murcia et al., 2016). Additionally,  
39 these methods should be easily transferable, allowing non-experts to collect data at large spatial

40 and temporal scales. Recent advances in remote sensing technologies and deep learning  
41 algorithms may provide the tools required for restoration practitioners (Brodrick et al., 2019;  
42 Kattenborn et al., 2021; Zhu et al., 2017). The work presented here demonstrates that using  
43 standard and low-cost “out-of-the-box” Unoccupied Aerial Vehicles (UAVs) coupled with  
44 Convolutional Neural Network (CNN) algorithms allows for the detection and quantification of  
45 *Portulacaria afra* Jacq. in restoration plots established between 2007 and 2008. *P. afra* is  
46 regarded as an ecosystem engineer in the Albany Subtropical Thicket biome (van Luijk et al.  
47 2013; Wilman et al. 2014), endemic to South Africa, and is the target species for large scale  
48 restoration initiatives (Mills et al., 2015; Mills and Cowling, 2006; van der Vyver et al., 2021a). It  
49 is estimated that up to 1.2 million hectares of the thicket biome exhibits some level of  
50 degradation (Lloyd et al., 2002) and in need of restoration intervention. With approximately 7000  
51 ha of plantings completed by 2017 (Mills and Robson, 2017), it is likely that the scale of thicket  
52 restoration will reach the tens of thousands of hectares in coming years. Thus, the monitoring  
53 tool presented here could prove invaluable to the rapid monitoring and management of thicket  
54 restoration initiatives.

55 The thicket biome is largely confined to the Eastern Cape Province of South Africa and is  
56 characterized as a low growing, spinescent, dense woodland system with high standing  
57 biomass often dominated by a matrix of the succulent tree, *P. afra* (Vlok et al., 2003). Occurring  
58 within a semi-arid environment, the high productivity of thicket is globally unique, with litter  
59 production rates comparable to that of some temperate forest systems (Lechmere-Oertel et al.,  
60 2008). This productivity formed the basis for wool, and mohair production in the region (Beinart,  
61 2008; Oakes, 1973; Stuart-Hill, 1992)s. While resistant to herbivory by indigenous browsers  
62 (Stuart-Hill, 1992, but see Landman et al., 2012), thicket vegetation is prone to *P. afra*  
63 denudation (due to the species' high palatability) when subjected to prolonged periods of  
64 browsing by domestic livestock (Hoffman and Cowling, 1990; Lechmere-Oertel et al., 2008).  
65 This results in a structural shift from a dense, closed-canopy woodland to an open habitat  
66 consisting of a handful of remnant and isolated woody species that occur within a matrix of bare  
67 soil, ephemeral herbs, grasses and dwarf shrubs (Lechmere-Oertel et al., 2008; Sigwela et al.,  
68 2009; Stuart-Hill, 1992).

69 The change in *P. afra* abundance due to unsustainable browsing practices pushes the system  
70 to a point where the natural regeneration (seed set and asexual reproduction via rooted lateral  
71 branches) of this species becomes insufficient to overcome rates of canopy reduction and  
72 mortality (Lechmere-Oertel et al., 2008). The environmental buffering effects of *P. afra* improves  
73 soil organic matter (Lechmere-Oertel et al., 2008) and water infiltration (Mills and de Wet, 2019;  
74 van Luijk et al., 2013) required for the recruitment of canopy tree species (Sigwela et al., 2009;  
75 Wilman et al., 2014), thus playing an important role in community assembly processes. The loss  
76 of *P. afra* cover, therefore, triggers a series of feedback loops that set the ecosystem onto a  
77 trajectory towards degradation: the lack of vegetation cover exposes the soils to erosion,  
78 depleting carbon stocks (Cowling and Mills, 2011; Lechmere-Oertel et al., 2008, 2005; Mills and  
79 Fey, 2004), which in turn disrupts hydrological processes such as water infiltration and retention  
80 (Cowling and Mills, 2011; Mills and de Wet, 2019; van Luijk et al., 2013), leading to further  
81 disruption of ecological functioning and ultimately biodiversity loss (Fabricius et al., 2003;  
82 Sigwela et al., 2009).

83 Active restoration of degraded *P. afra* thicket has been sponsored, at a landscape scale, by the

84 South African Government, in an initiative called the Subtropical Thicket Restoration Project  
85 (STRP). This aims to generate employment opportunities that will, ultimately, be funded by the  
86 global carbon market (Marais et al., 2009). The high productivity of *P. afra* thicket coupled with  
87 the ease of propagation (i.e. through the planting of unrooted *P. afra* truncheons into degraded  
88 habitat: Mills and Cowling, 2006; van der Vyver et al., 2021), lends the vegetation type well to  
89 carbon credit generation, sequestering up to 15.4 t CO<sub>2</sub> ha<sup>-1</sup> yr<sup>-1</sup> (Mills and Cowling, 2014).  
90 However, restoration success and carbon sequestration are measured over decades, while  
91 implementation success and restoration trajectories must be monitored over shorter time spans  
92 to allow for adaptive management. This monitoring is often limited to field measures that are  
93 time- and labour-intensive when having to cover hundreds to thousands of hectares. However,  
94 recent technological advancements have increased the availability of remote sensing data,  
95 providing solutions to this challenge in restoration (Almeida et al., 2021; Chen et al., 2021;  
96 Wang et al., 2021).  
97 Novel aerial imagery platforms, such as UAVs, make the generation of high-resolution remote  
98 sensing data rapidly available with relatively little sampling effort (Colomina and Molina, 2014).  
99 These platforms require little specialist training and can provide high resolution data at spatial  
100 and temporal scales. Given the accelerated availability and volumes of such data, automated  
101 approaches are required to harness their full potential (Kattenborn et al., 2021). Convolutional  
102 Neural Networks (CNNs) are particularly well suited to the analysis of vegetation, due to this  
103 class of algorithms being designed to extract features in data (spatial features in the case of  
104 aerial imagery) that best describe the target object (e.g. leaf and canopy shapes, edges  
105 between individuals, and individual species spectral properties). Training the model to extract  
106 the desired features is particularly efficient as the algorithm itself is able to learn what patterns  
107 are important based on the reference material. This is done in sequential batches, enabling the  
108 model to cope with large amounts of data, which facilitates the training of models that are  
109 transferable across sites and remote sensing data conditions. CNNs have thus been applied in  
110 the identification of individual plant traits (e.g. growth form: Fromm et al., 2019 and Sylvain et  
111 al., 2019; and plant phenology: Hasan et al., 2018), species (Fricker et al., 2019 and Wagner et  
112 al., 2020), and communities (Kattenborn et al., 2019) from aerial imagery.

113 The growing interest in the global carbon market presents restoration initiatives with novel  
114 funding structures (Galatowitsch, 2009), that are likely to contribute to the upscaling of thicket  
115 restoration initiatives (Marais et al., 2009; Mills et al., 2015). This upscaling will require effective  
116 means of monitoring change in canopy cover, at a range of spatial and temporal scales, to  
117 inform adaptive management practices. By coupling imagery derived from readily available “out-  
118 of-the-box” UAV’s and CNN segmentation algorithms, this work successfully classifies canopy  
119 cover of reintroduced *P. afra* in experimental thicket restoration plots established between 2008  
120 and 2009 (Mills et al., 2015). This demonstrates that commercially available UAVs coupled with  
121 CNN algorithms can provide rapid and accurate estimates of *P. afra* cover for restoration  
122 initiatives at low cost and without expert training. Implementation of this monitoring approach will  
123 allow for the rapid monitoring of changes in vegetation cover and facilitate adaptive  
124 management by allowing fine-scaled temporal monitoring of restoration sites.

## 125 **Materials & Methods**

## 126 **Study site and UAV data acquisition**

127 A total of 300 experimental restoration plots were established in degraded habitat across the  
128 global extent of *P. afra* dominated thicket vegetation (as delineated by Vlok et al., 2003). Each  
129 plot consisted of a 0.25 ha (50 x 50 m) herbivore enclosure that was fenced to a height of 1.2 m.  
130 These experimental plots tested a range of *P. afra* planting strategies (briefly described in van  
131 der Vyver et al., 2021), but produced highly variable results, with survival ranging between 0 -  
132 100% between plots (Mills and Robson, 2017; van der Vyver et al., 2021b). Furthermore, the  
133 complete or partial removal of fencing exposed some experimental plots to herbivory (van der  
134 Vyver et al., 2021a), and differences in local climatic and soil conditions (Vlok et al., 2003) may  
135 have resulted in differences in the rate of *P. afra* growth. Thus, *P. afra* cover is highly variable  
136 between these plots. Aerial imagery for thirty-two experimental plots that reflect this variability in  
137 *P. afra* cover was acquired to train and test the CNN based segmentation models.

138 For this, RGB imagery was acquired in thirty-two individual flights in 2020-2021 using a DJI  
139 Phantom 4 Pro (n = 12) and DJI Mavic 2 Pro (n = 20). The imagery was acquired at different  
140 times and dates. This resulted in very diverse image properties, such as image brightness,  
141 contrast, or the presence, orientation and size of cast shadows. The flying height was 30 m  
142 above ground, with 10 m spacing between photographs, and this resulted in a Ground Sampling  
143 Distance (GSD) of ~0.9cm/pixel. Flight plans were generated using a custom script in R  
144 (V1.4.1717), and FlyLitchi (V4.22, www.flylitchi.com) was used to operate the UAV during  
145 flights. Imagery was stitched using Metashape (V1.7.2, Agisoft LLC). Examples of the images  
146 generated are provided in Figure 1.

147 Reference data was generated by visual interpretation of the orthoimagery in a GIS  
148 environment, where *P. afra* crowns were delineated by means of manually geocoded polygons.  
149 For each orthoimage and plot, the reference data acquisition targeted an area of approximately  
150 12.5 by 12.5 m. After visual interpretation, the shapefiles were converted to a binary mask  
151 (presence vs. absence of *P. afra*) with a raster resolution corresponding to the respective  
152 orthoimage.

## 153 **CNN model training and validation**

154 For training the CNN, non-overlapping tile pairs of 128 by 128 pixels were seamlessly cropped  
155 from the orthoimages (predictors) and the masks (reference). For this, only the visually  
156 interpreted (*P. afra* cover) portion of the reference images was considered (cf. previous section).  
157 As a segmentation algorithm, we implemented the Unet architecture (Ronneberger et al., 2015).  
158 The Unet architecture is composed of an encoder and a decoder part, which are linked with skip  
159 connection. Both the encoder and decoder parts contain pooling operations, which reduce the  
160 spatial resolution of the feature maps. In the encoder part, the model extracts the image  
161 features for detecting *P. afra* at multiple spatial scales. The skip-connections transfer the  
162 activation maps of each spatial scale to the decoder part, which, hence, enables segmentation  
163 of the crown dimensions at the original spatial resolution of the input imagery. Here, we used  
164 encoder and decoder parts composed of 4 convolutional blocks, where each block consists of  
165 two convolutional layers followed by a batch normalization and max pooling operation. As  
166 activation functions, we used Gaussian Error Linear Units (GELU). Similar setups have been  
167 successfully applied in previous studies (Kattenborn et al., 2019; Schiefer et al., 2020).  
168 To avoid optimistic model evaluation by spatially autocorrelated training and validation data  
169 (Ploton et al. 2021), we randomly split all available data on a plot basis, where a portion of plots

170 was used for model training (n=24) and model testing (n=8). The training data was again split in  
171 training (7/8) and validation data (1/8), whereas the validation data was used to monitor the  
172 training process. The models were trained in 100 epochs and the final model used for further  
173 analysis was selected based on the lowest loss on the validation data. As a loss function, we  
174 used the binary cross-entropy. Training the model took about 457 minutes using an NVIDIA  
175 A6000. The final model performance for the tiles that were included in the training, validation  
176 and testing was reported using the F1-score (also known as dice coefficient). Additionally, we  
177 performed a t-Test to assess if F1-scores differed significantly between imagery obtained with  
178 the DJI Phantom 4 Pro and the DJI Mavic 2 Pro.

179 The final model was used to predict *P. afra* crowns in all orthoimagery. The prediction was  
180 performed using a moving window approach, in which individual tiles of the same size as used  
181 for model training (128 x 128 pixels) were seamlessly cropped from the orthoimagery. The final  
182 model was then applied on these tiles and the predictions were stored as a prediction raster  
183 containing the class probability (0 = absence & 1 = presence of *P. afra*). To reduce edge effects  
184 (potential mispredictions at the border of tiles), we applied this procedure two times, where the  
185 locations of extracting the tiles were shifted by 50 % of the tile size (64 pixels). The two resulting  
186 prediction rasters were averaged and a threshold of (0.5) was applied to produce a binary  
187 classification output.

## 188 Results

189 The model performance in terms of F1-score was 0.932 for the training data, 0.926 for the  
190 validation data and 0.936 for the test data obtained from the entirely independent plots. The F1-  
191 score for most individual plots was at least 0.9 (n = 29), 3 plots with F1-scores lower than 0.9  
192 were observed. The lower accuracy of two of these plots resulted from misinterpretations of the  
193 reference data and in one case from false-positive predictions in very dark and large cast  
194 shadows. No significant difference in F1-scores was detected between predictions obtained for  
195 the DJI Phantom 4 Pro and the DJI Mavic 2 Pro (t = 1.5283, df = 24.84, p-value = 0.1391,  
196 Figure 2).

## 197 Discussion

198 The application of CNN machine learning models proved suitable for the classification and  
199 quantification of *P. afra* cover in the heterogenous RGB aerial imagery, generated from  
200 commercially available 'out of the box' UAV models (Figure 3). The method presented here  
201 proved to be transferable across different UAV models, sites and illumination conditions with no  
202 apparent loss of performance (Figure 2).

203 Where multiple UAV flights are required for data collection, it is common practice to limit flights  
204 to the same time of day and on clear days so as to minimize the potential effects of solar angle  
205 and radiance on model performance (Abdulridha et al., 2019; Adak et al., 2021; Eskandari et al.,  
206 2020; Guo et al., 2020; Lopatin et al., 2019). This was not the case here, UAV data acquisition  
207 was not restricted to specific illumination conditions, no image corrections or cross-calibrations  
208 were conducted, and the model was trained using images sourced under a range of conditions  
209 and using different models of UAV's. Despite this, model performance was comparable to other  
210 studies (see studies reviewed in Kattenborn et al., 2021), highlighting the robust nature of the  
211 CNN model applied, which should, therefore, be easily transferable for the quantification of *P.*  
212 *afra* cover in restoration sites across the Albany Thicket biome in South Africa.

213 The ease of use and transferability of aerial image classification models presents new

214 opportunities for defining and tracking restoration targets across a range of spatial and temporal  
215 scales. Loewensteiner et al. (2021) demonstrate the importance of temporal scale in defining  
216 restoration targets, applying CNN models to the classification of woody cover in a Savanna  
217 ecosystem over a 66 year time period. Woody cover was found to be variable over time, thus,  
218 restoration targets for the system should fall within a spectrum of woody cover and are not  
219 required to reflect the current state of the reference ecosystem. A similar approach could be  
220 applied to describe restoration targets and planting densities in thicket restoration, as the  
221 current practice aims to generate a dense closed canopy with individual *P. afra* reintroduced at  
222 high densities (1-2 m spacing). Additionally, it may be possible to detect return of ecosystem  
223 functioning using aerial imagery. This may include measures of structural complexity, indicative  
224 of biodiversity returns (Camarretta et al., 2020), or regeneration dynamics (e.g. measures of  
225 target species cover as presented here for *P. afra*) and seedling recruitment (Buters et al., 2019;  
226 Fromm et al., 2019).

227 The application of the model presented here will allow thicket restoration initiatives to rapidly  
228 collect data from a range of different UAV models for temporal monitoring of restoration  
229 trajectories, informing adaptive management practices (Camarretta et al., 2020). This currently  
230 presents a major challenge in thicket restoration as field-based monitoring often takes place in  
231 distant rural areas, where *P. afra* has coalesced to form a fairly impenetrable barrier of  
232 vegetation, and requires expert training in ecological monitoring techniques. Repeat aerial  
233 imagery can be generated, by almost anyone with a little training, for restoration sites with no  
234 increase in sampling effort over time. The data generated can potentially be sent to a  
235 centralised repository for analysis, bridging the science-practice gap (Dickens and Suding,  
236 2013) and promoting further collaboration within the Albany Subtropical Thicket restoration  
237 community (Mills et al., 2015). This will provide managers with estimates of plant density (using  
238 blob detection, which separates individuals in the CNN classification: Kattenborn et al., 2021);  
239 accurate estimates of plant survival in the first year of implementation (comparing plant density  
240 changes between flights); and estimates of plant cover changes overtime to ensure  
241 interventions can be made if plant cover is lost due to disturbance (e.g. frost: Duker et al. 2015,  
242 or herbivory: van der Vyver et al. 2021). In such cases, actions can be informed by the scientific  
243 community and implemented by managers and landowners to remediate the processes  
244 threatening the restoration initiative.

245 Aerial imagery-based monitoring is well suited to collecting data at spatial scales relevant to  
246 ecosystem restoration. The spatial extent to which a UAV can collect data is confined by the  
247 battery life (flight time), whereas the classification of these images using CNN models has the  
248 potential to classify vegetation dynamics at large spatial scales (Flood et al., 2019; Timilsina et  
249 al., 2020). Cloud computing provides a possible means of overcoming the computational load of  
250 processing large data (see Kattenborn et al. 2021 for a summary of available servers for CNN  
251 data analysis), making the classification of large spatial areas feasible for a greater number of  
252 practitioners. This may prove invaluable for the upscaling of thicket restoration in South Africa,  
253 with an estimated 1.2 million ha of degraded ecosystems having some restoration potential  
254 (Lloyd et al., 2002).

255 While we have presented the first CNN model relevant to the restoration of the Albany  
256 Subtropical Thicket biome, and that could be applied to monitoring restoration at scale, we do  
257 not harness the full capabilities of machine learning in this study. Here, we used the well-known

258 Unet algorithm (Ronneberger et al., 2015), while CNN-based segmentation algorithms are  
259 steadily advancing (Minaee et al., 2021). Likewise, UAV and sensor technology continue to  
260 advance, improved image resolution and spectral range of drone imagery are likely to come at  
261 lower prices, making detection of finer scaled patterns possible without having to decrease flight  
262 altitudes. Additionally, the three-dimensional mapping of vegetation cover using LiDAR  
263 technologies provides opportunities to estimate plant biomass without labour intensive fieldwork  
264 (Shendryk et al., 2020; ten Harkel et al., 2019). This may aid in estimating carbon sequestration  
265 in restoration sites to assist in carbon credit verification and issuing for the global carbon  
266 market. Harris et al. (2021) present an example of this, reporting a significant correlation  
267 between above-ground carbon estimates calculated from remote sensed *P. afra* canopies and  
268 field measures. Increased image resolution can provide novel insights into *P. afra* recruitment  
269 dynamics, and further developing the CNN model to classify multiple species (as per Fricker et  
270 al., 2019 and Kattenborn et al., 2019) can provide insights into biodiversity return with relatively  
271 low sampling effort (a laborious task to complete using manual field measures, last undertaken  
272 by van der Vyver et al., 2013). Thus, it is evident that the work present here should inspire  
273 future application of UAV imagery to the ecology and management of Albany Subtropical  
274 Thicket vegetation.

## 275 **Conclusions**

276 Recent advancements in machine learning and remote sensing technologies have provided  
277 unprecedented access to, and automated processing of earth imagery. This can potentially  
278 transform monitoring of ecosystem restoration practices, shifting protocols from time and  
279 resource exhaustive field measures to remote sensing approaches. Here we demonstrated the  
280 utility of standard 'out of the box' UAV data coupled with CNN models to classify and quantify *P.*  
281 *afra* cover in thicket restoration plots. The models were transferable across different plot  
282 properties, illumination conditions, and UAV models. The integration of this model in the  
283 monitoring of thicket restoration will aid in the planned upscaling of Albany Subtropical Thicket  
284 restoration and generate valuable temporal data for evaluating restoration trajectories and  
285 demographic processes. This will promote collaborative efforts between scientists and  
286 practitioners, strengthening the restoration community. Importantly, the integration of this  
287 monitoring approach does not require any technical knowledge of the CNN model, or special  
288 skill sets to fly commercially available UAVs, and can thus reduce the sampling effort required  
289 for monitoring restoration at scale.

## 290 **Acknowledgements**

291 The authors would like to thank Dr Marius L. van der Vyver for his assistance in acquiring UAV  
292 imagery and the student interns (Anize Tempel, Kristen Hunt and Oyena Masiko) that assisted  
293 in manual classification of images for model training.

## 294 **References**

- 295 Abdulridha, J., Batuman, O., Ampatzidis, Y., 2019. UAV-Based remote sensing technique to  
296 detect citrus canker disease utilizing hyperspectral imaging and machine learning.  
297 Remote Sens. 11, 1373. <https://doi.org/10.3390/rs11111373>
- 298 Adak, A., Murray, S.C., Božinović, S., Lindsey, R., Nakasagga, S., Chatterjee, S., Anderson,  
299 S.L., Wilde, S., 2021. Temporal vegetation indices and plant height from remotely  
300 sensed imagery can predict grain yield and flowering time breeding value in maize via

- 301 machine learning regression. *Remote Sens.* 13, 2141.  
302 <https://doi.org/10.3390/rs13112141>
- 303 Almeida, D.R.A. de, Broadbent, E.N., Ferreira, M.P., Meli, P., Zambrano, A.M.A., Gorgens, E.B.,  
304 Resende, A.F., de Almeida, C.T., do Amaral, C.H., Corte, A.P.D., Silva, C.A., Romanelli,  
305 J.P., Prata, G.A., de Almeida Papa, D., Stark, S.C., Valbuena, R., Nelson, B.W.,  
306 Guillemot, J., Féret, J.-B., Chazdon, R., Brancalion, P.H.S., 2021. Monitoring restored  
307 tropical forest diversity and structure through UAV-borne hyperspectral and lidar fusion.  
308 *Remote Sens. Environ.* 264, 112582. <https://doi.org/10.1016/j.rse.2021.112582>
- 309 Beinart, W., 2008. The rise of conservation in South Africa: settlers, livestock, and the  
310 environment; 1770 - 1950, 1. publ. in pbk. ed. Oxford University Press, Oxford.
- 311 Brodrick, P.G., Davies, A.B., Asner, G.P., 2019. Uncovering ecological patterns with  
312 convolutional neural networks. *Trends Ecol. Evol.* 34, 734–745.  
313 <https://doi.org/10.1016/j.tree.2019.03.006>
- 314 Buters, Belton, Cross, 2019. Seed and seedling detection using unmanned aerial vehicles and  
315 automated image classification in the monitoring of ecological recovery. *Drones* 3, 53.  
316 <https://doi.org/10.3390/drones3030053>
- 317 Camarretta, N., Harrison, P.A., Bailey, T., Potts, B., Lucieer, A., Davidson, N., Hunt, M., 2020.  
318 Monitoring forest structure to guide adaptive management of forest restoration: a review  
319 of remote sensing approaches. *New For.* 51, 573–596. <https://doi.org/10.1007/s11056-019-09754-5>
- 320
- 321 Chen, A., Yang, X., Guo, J., Xing, X., Yang, D., Xu, B., 2021. Synthesized remote sensing-  
322 based desertification index reveals ecological restoration and its driving forces in the  
323 northern sand-prevention belt of China. *Ecol. Indic.* 131, 108230.  
324 <https://doi.org/10.1016/j.ecolind.2021.108230>
- 325 Colomina, I., Molina, P., 2014. Unmanned aerial systems for photogrammetry and remote  
326 sensing: A review. *ISPRS J. Photogramm. Remote Sens.* 92, 79–97.  
327 <https://doi.org/10.1016/j.isprsjprs.2014.02.013>
- 328 Cowling, R.M., Mills, A.J., 2011. A preliminary assessment of rain throughfall beneath  
329 *Portulacaria afra* canopy in subtropical thicket and its implications for soil carbon stocks.  
330 *South Afr. J. Bot.* 77, 236–240. <https://doi.org/10.1016/j.sajb.2010.06.004>
- 331 de Almeida, D.R.A., Stark, S.C., Valbuena, R., Broadbent, E.N., Silva, T.S.F., de Resende, A.F.,  
332 Ferreira, M.P., Cardil, A., Silva, C.A., Amazonas, N., Zambrano, A.M.A., Brancalion,  
333 P.H.S., 2020. A new era in forest restoration monitoring. *Restor. Ecol.* 28, 8–11.  
334 <https://doi.org/10.1111/rec.13067>
- 335 Dickens, S.J.M., Suding, K.N., 2013. Spanning the science-practice divide: why restoration  
336 scientists need to be more involved with practice. *Ecol. Restor.* 31, 134–140.  
337 <https://doi.org/10.3368/er.31.2.134>
- 338 Duker, R., Cowling, R.M., du Preez, D.R., Potts, A.J., 2015. Frost, *Portulacaria afra* Jacq., and  
339 the boundary between the Albany Subtropical Thicket and Nama-Karoo biomes. *South*  
340 *Afr. J. Bot.* 101, 112–119. <https://doi.org/10.1016/j.sajb.2015.05.004>
- 341 Eskandari, R., Mahdianpari, M., Mohammadimanesh, F., Salehi, B., Brisco, B., Homayouni, S.,  
342 2020. Meta-analysis of unmanned aerial vehicle (UAV) imagery for agro-environmental  
343 monitoring using machine learning and statistical models. *Remote Sens.* 12, 3511.  
344 <https://doi.org/10.3390/rs12213511>

- 345 Fabricius, C., Burger, M., Hockey, P. a. R., 2003. Comparing biodiversity between protected  
346 areas and adjacent rangeland in xeric succulent thicket, South Africa: arthropods and  
347 reptiles. *J. Appl. Ecol.* 40, 392–403. <https://doi.org/10.1046/j.1365-2664.2003.00793.x>
- 348 Flood, N., Watson, F., Collett, L., 2019. Using a U-net convolutional neural network to map  
349 woody vegetation extent from high resolution satellite imagery across Queensland,  
350 Australia. *Int. J. Appl. Earth Obs. Geoinformation* 82, 101897.  
351 <https://doi.org/10.1016/j.jag.2019.101897>
- 352 Fricker, G.A., Ventura, J.D., Wolf, J.A., North, M.P., Davis, F.W., Franklin, J., 2019. A  
353 convolutional neural network classifier identifies tree species in mixed-conifer forest from  
354 hyperspectral imagery. *Remote Sens.* 11, 2326. <https://doi.org/10.3390/rs11192326>
- 355 Fromm, M., Schubert, M., Castilla, G., Linke, J., McDermid, G., 2019. Automated detection of  
356 conifer seedlings in drone imagery using convolutional neural networks. *Remote Sens.*  
357 11, 2585. <https://doi.org/10.3390/rs11212585>
- 358 Galatowitsch, S.M., 2009. Carbon offsets as ecological restorations. *Restor. Ecol.* 17, 563–570.  
359 <https://doi.org/10.1111/j.1526-100X.2009.00587.x>
- 360 Guo, Y., Yin, G., Sun, H., Wang, H., Chen, S., Senthilnath, J., Wang, J., Fu, Y., 2020. Scaling  
361 effects on chlorophyll content estimations with RGB camera mounted on a UAV platform  
362 using machine-learning methods. *Sensors* 20, 5130. <https://doi.org/10.3390/s20185130>
- 363 Harris, D., Bolus, C., Reeler, J., 2021. Very high resolution aboveground carbon mapping in  
364 subtropical thicket. *J. Appl. Remote Sens.* 15. <https://doi.org/10.1117/1.JRS.15.038502>
- 365 Hasan, M.M., Chopin, J.P., Laga, H., Miklavcic, S.J., 2018. Detection and analysis of wheat  
366 spikes using Convolutional Neural Networks. *Plant Methods* 14, 100.  
367 <https://doi.org/10.1186/s13007-018-0366-8>
- 368 Hoffman, M.T., Cowling, R.M., 1990. Desertification in the lower Sundays River Valley, South  
369 Africa. *J. Arid Environ.* 19, 105–118. [https://doi.org/10.1016/S0140-1963\(18\)30834-6](https://doi.org/10.1016/S0140-1963(18)30834-6)
- 370 Kattenborn, T., Eichel, J., Fassnacht, F.E., 2019. Convolutional Neural Networks enable  
371 efficient, accurate and fine-grained segmentation of plant species and communities from  
372 high-resolution UAV imagery. *Sci. Rep.* 9, 17656. <https://doi.org/10.1038/s41598-019-53797-9>
- 373
- 374 Kattenborn, T., Leitloff, J., Schiefer, F., Hinz, S., 2021. Review on Convolutional Neural  
375 Networks (CNN) in vegetation remote sensing. *ISPRS J. Photogramm. Remote Sens.*  
376 173, 24–49. <https://doi.org/10.1016/j.isprsjprs.2020.12.010>
- 377 Landman, M., Schoeman, D.S., Hall-Martin, A.J., Kerley, G.I.H., 2012. Understanding Long-  
378 Term Variations in an Elephant Piosphere Effect to Manage Impacts. *PLoS ONE* 7,  
379 e45334. <https://doi.org/10.1371/journal.pone.0045334>
- 380 Lechmere-Oertel, R.G., Kerley, G.I.H., Cowling, R.M., 2005. Patterns and implications of  
381 transformation in semi-arid succulent thicket, South Africa. *J. Arid Environ.* 62, 459–474.  
382 <https://doi.org/10.1016/j.jaridenv.2004.11.016>
- 383 Lechmere-Oertel, R.G., Kerley, G.I.H., Mills, A.J., Cowling, R.M., 2008. Litter dynamics across  
384 browsing-induced fence-line contrasts in succulent thicket, South Africa. *South Afr. J.*  
385 *Bot.* 74, 651–659. <https://doi.org/10.1016/j.sajb.2008.04.002>
- 386 Lloyd, J.W., van den Berg, E.C., Palmer, A.R., 2002. Patterns of Transformation and Degradation in the Thicket  
387 Biome, South Africa, TERU Report (No. 39). University of Port Elizabeth.
- 388 Lloyd, J.W., van den Berg, E.C. & Palmer, A.R. 2002. Patterns of transformation and

- 389 degradation in the thicket biome, South Africa. Port Elizabeth, TERU Report 39,  
390 University of Port Elizabeth.
- 391 Loewensteiner, D.A., Bartolo, R.E., Whiteside, T.G., Esparon, A.J., Humphrey, C.L., 2021.  
392 Measuring savanna woody cover at scale to inform ecosystem restoration. *Ecosphere*  
393 12. <https://doi.org/10.1002/ecs2.3437>
- 394 Lopatin, J., Dolos, K., Kattenborn, T., Fassnacht, F.E., 2019. How canopy shadow affects  
395 invasive plant species classification in high spatial resolution remote sensing. *Remote*  
396 *Sens. Ecol. Conserv.* 5, 302–317. <https://doi.org/10.1002/rse2.109>
- 397 Marais, C., Cowling, R.M., Powell, M., Mills, A., 2009. Establishing the platform for a carbon  
398 sequestration market in South Africa: The Working for Woodlands Subtropical Thicket  
399 Restoration Programme. Presented at the XIII World Forestry Congress, Buenos Aires,  
400 Argentina, p. 13.
- 401 Méndez-Toribio, M., Martínez-Garza, C., Ceccon, E., 2021. Challenges during the execution,  
402 results, and monitoring phases of ecological restoration: Learning from a country-wide  
403 assessment. *PLOS ONE* 16, e0249573. <https://doi.org/10.1371/journal.pone.0249573>
- 404 Mills, A., Fey, M., 2004. Transformation of thicket to savanna reduces soil quality in the Eastern  
405 Cape, South Africa. *Plant Soil* 265, 153–163. <https://doi.org/10.1007/s11104-005-0534-2>
- 406 Mills, A., Vyver, M., Gordon, I., Patwardhan, A., Marais, C., Blignaut, J., Sigwela, A., Kgope, B.,  
407 2015. Prescribing innovation within a large-scale restoration programme in degraded  
408 subtropical thicket in South Africa. *Forests* 6, 4328–4348.  
409 <https://doi.org/10.3390/f6114328>
- 410 Mills, A.J., Cowling, R.M., 2014. How fast can carbon be sequestered when restoring degraded  
411 subtropical thicket?: Carbon sequestration in restored subtropical thicket. *Restor. Ecol.*  
412 22, 571–573. <https://doi.org/10.1111/rec.12117>
- 413 Mills, A.J., Cowling, R.M., 2006. Rate of carbon sequestration at two thicket restoration sites in  
414 the Eastern Cape, South Africa. *Restor. Ecol.* 14, 38–49. [https://doi.org/10.1111/j.1526-](https://doi.org/10.1111/j.1526-100X.2006.00103.x)  
415 [100X.2006.00103.x](https://doi.org/10.1111/j.1526-100X.2006.00103.x)
- 416 Mills, A.J., de Wet, R., 2019. Quantifying a sponge: The additional water in restored thicket.  
417 *South Afr. J. Sci.* 115. <https://doi.org/10.17159/sajs.2019/a0309>
- 418 Mills, A.J., Robson, A., 2017. Survivorship of spekboom (*Portulacaria afra*) planted within the  
419 Subtropical Thicket Restoration Programme. *South Afr. J. Sci.* 113.  
420 <https://doi.org/10.17159/sajs.2017/a0196>
- 421 Minaee, S., Boykov, Y.Y., Porikli, F., Plaza, A.J., Kehtarnavaz, N., Terzopoulos, D., 2021.  
422 Image segmentation using deep learning: A survey. *IEEE Trans. Pattern Anal. Mach.*  
423 *Intell.* 1–1. <https://doi.org/10.1109/TPAMI.2021.3059968>
- 424 Murcia, C., Guariguata, M.R., Andrade, Á., Andrade, G.I., Aronson, J., Escobar, E.M., Etter, A.,  
425 Moreno, F.H., Ramírez, W., Montes, E., 2016. Challenges and prospects for scaling-up  
426 ecological restoration to meet international commitments: Colombia as a case study:  
427 scaling-up ecological restoration in Colombia. *Conserv. Lett.* 9, 213–220.  
428 <https://doi.org/10.1111/conl.12199>
- 429 Oakes, A.J., 1973. *Portulacaria afra* Jacq. — A potential browse plant. *Econ. Bot.* 27, 413–416.  
430 <https://doi.org/10.1007/BF02860694>
- 431 Ronneberger, O., Fischer, P., Brox, T., 2015. U-Net: Convolutional Networks for biomedical  
432 image segmentation, in: Navab, N., Hornegger, J., Wells, W.M., Frangi, A.F. (Eds.),

- 433 Medical image computing and computer-assisted intervention – MICCAI 2015, Lecture  
434 Notes in Computer Science. Springer International Publishing, Cham, pp. 234–241.  
435 [https://doi.org/10.1007/978-3-319-24574-4\\_28](https://doi.org/10.1007/978-3-319-24574-4_28)
- 436 Schiefer, F., Kattenborn, T., Frick, A., Frey, J., Schall, P., Koch, B., Schmidlein, S., 2020.  
437 Mapping forest tree species in high resolution UAV-based RGB-imagery by means of  
438 convolutional neural networks. ISPRS J. Photogramm. Remote Sens. 170, 205–215.
- 439 Shendryk, Y., Sofonia, J., Garrard, R., Rist, Y., Skocaj, D., Thorburn, P., 2020. Fine-scale  
440 prediction of biomass and leaf nitrogen content in sugarcane using UAV LiDAR and  
441 multispectral imaging. Int. J. Appl. Earth Obs. Geoinformation 92, 102177.  
442 <https://doi.org/10.1016/j.jag.2020.102177>
- 443 Sigwela, A.M., Kerley, G.I.H., Mills, A.J., Cowling, R.M., 2009. The impact of browsing-induced  
444 degradation on the reproduction of subtropical thicket canopy shrubs and trees. South  
445 Afr. J. Bot. 75, 262–267. <https://doi.org/10.1016/j.sajb.2008.12.001>
- 446 Stuart-Hill, G. C., 1992. Effects of elephants and goats on the kaffrarian succulent thicket of the  
447 Eastern Cape, South Africa. J. Appl. Ecol. 29, 699. <https://doi.org/10.2307/2404479>
- 448 Sylvain, J.-D., Drolet, G., Brown, N., 2019. Mapping dead forest cover using a deep  
449 convolutional neural network and digital aerial photography. ISPRS J. Photogramm.  
450 Remote Sens. 156, 14–26. <https://doi.org/10.1016/j.isprsjprs.2019.07.010>
- 451 ten Harkel, J., Bartholomeus, H., Kooistra, L., 2019. Biomass and crop height estimation of  
452 different crops using UAV-based lidar. Remote Sens. 12, 17.  
453 <https://doi.org/10.3390/rs12010017>
- 454 Timilsina, S., Aryal, J., Kirkpatrick, J.B., 2020. Mapping urban tree cover changes using Object-  
455 Based Convolution Neural Network (OB-CNN). Remote Sens. 12, 3017.  
456 <https://doi.org/10.3390/rs12183017>
- 457 van der Vyver, M.L., Cowling, R.M., Mills, A.J., Difford, M., 2013. Spontaneous return of  
458 biodiversity in restored subtropical thicket: *Portulacaria afra* as an ecosystem engineer:  
459 spekboom restoration also restores biodiversity. Restor. Ecol. 21, 736–744.  
460 <https://doi.org/10.1111/rec.12000>
- 461 van der Vyver, M.L., Mills, A.J., Cowling, R.M., 2021a. A biome-wide experiment to assess the  
462 effects of propagule size and treatment on the survival of *Portulacaria afra* (spekboom)  
463 truncheons planted to restore degraded subtropical thicket of South Africa. PLOS ONE  
464 16, e0250256. <https://doi.org/10.1371/journal.pone.0250256>
- 465 van der Vyver, M.L., Mills, A.J., Difford, M., Cowling, R.M., 2021b. Herbivory and  
466 misidentification of target habitat constrain region-wide restoration success of spekboom  
467 (*Portulacaria afra*) in South African subtropical succulent thicket. PeerJ 9, e11944.  
468 <https://doi.org/10.7717/peerj.11944>
- 469 van Luijk, G., Cowling, R.M., Riksen, M.J.P.M., Glenday, J., 2013. Hydrological implications of  
470 desertification: Degradation of South African semi-arid subtropical thicket. J. Arid  
471 Environ. 91, 14–21. <https://doi.org/10.1016/j.jaridenv.2012.10.022>
- 472 Vlok, J.H.J., Euston-Brown, D.I.W., Cowling, R.M., 2003. Acocks' Valley Bushveld 50 years on:  
473 new perspectives on the delimitation, characterisation and origin of subtropical thicket  
474 vegetation. South Afr. J. Bot. 69, 27–51. [https://doi.org/10.1016/S0254-6299\(15\)30358-6](https://doi.org/10.1016/S0254-6299(15)30358-6)

- 475 Wagner, F.H., Sanchez, A., Aidar, M.P., Rochelle, A.L., Tarabalka, Y., Fonseca, M.G., Phillips,  
476 O.L., Gloor, E. and Aragao, L.E., 2020. Mapping Atlantic rainforest degradation and  
477 regeneration history with indicator species using convolutional network. *PloS one*, 15(2),  
478 p.e0229448. <https://doi.org/10.1371/journal.pone.0229448>
- 479 Wang, H., Xie, M., Li, H., Feng, Q., Zhang, C., Bai, Z., 2021. Monitoring ecosystem restoration  
480 of multiple surface coal mine sites in China via LANDSAT images using the Google  
481 Earth Engine. *Land Degrad. Dev.* 32, 2936–2950. <https://doi.org/10.1002/ldr.3914>
- 482 Wilman, V., Campbell, E.E., Potts, A.J., Cowling, R.M., 2014. A mismatch between germination  
483 requirements and environmental conditions: Niche conservatism in xeric subtropical  
484 thicket canopy species? *South Afr. J. Bot.* 92, 1–6.  
485 <https://doi.org/10.1016/j.sajb.2013.12.007>
- 486 Zhu, X.X., Tuia, D., Mou, L., Xia, G.-S., Zhang, L., Xu, F., Fraundorfer, F., 2017. Deep learning  
487 in remote sensing: A comprehensive review and list of resources. *IEEE Geosci. Remote*  
488 *Sens. Mag.* 5, 8–36. <https://doi.org/10.1109/MGRS.2017.2762307>

# Figure 1

Photographs of three experimental restoration plots.

(A-C) Experimental restoration plots in context. Note the open woodland (degraded thicket) surrounding the plots in relation to the dense woodland (intact thicket) in the background.

(D-F) Aerial images of the above restoration plots used for *P. afra* canopy cover classification.

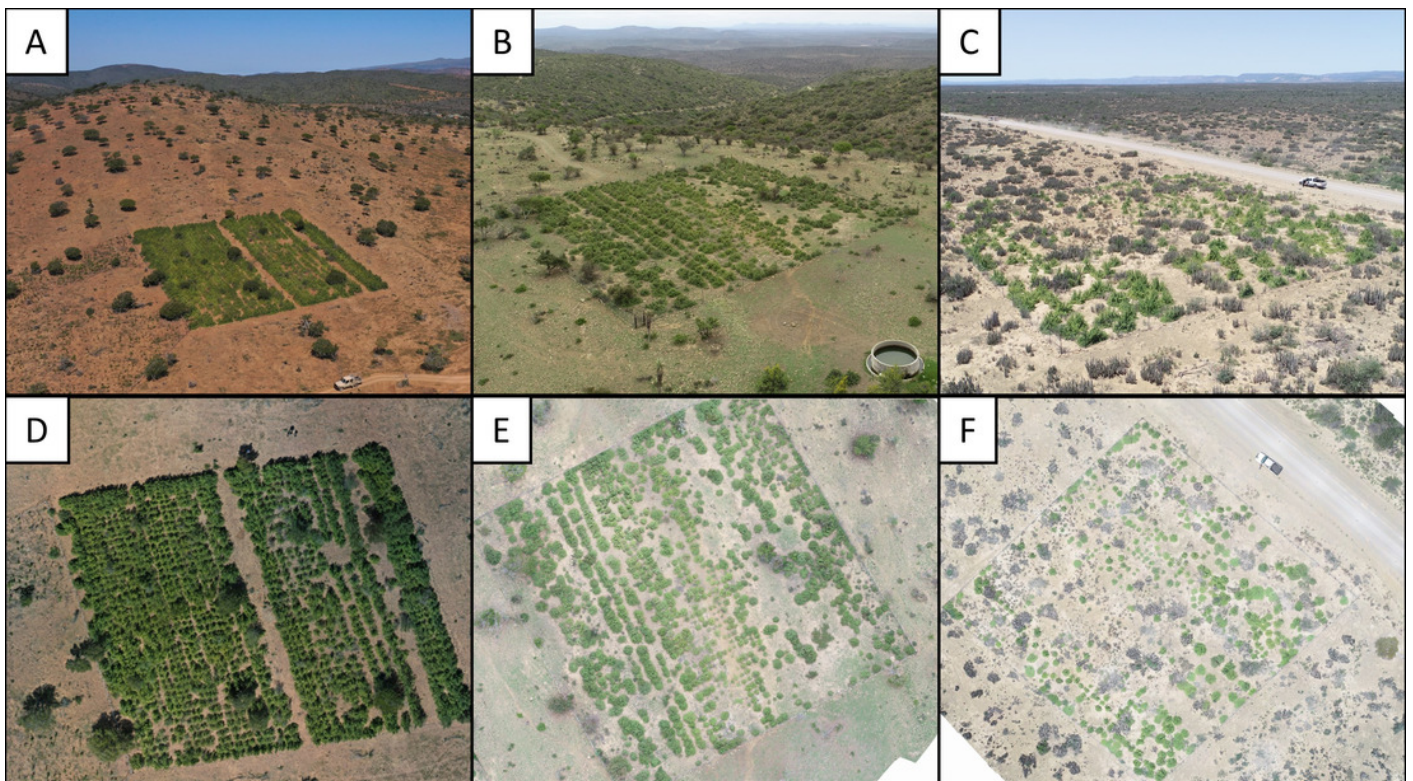


## Figure 2

Model performance estimates using F1-scores, (train) Training data, (val) the validation data and (test) data of entirely independent plots.

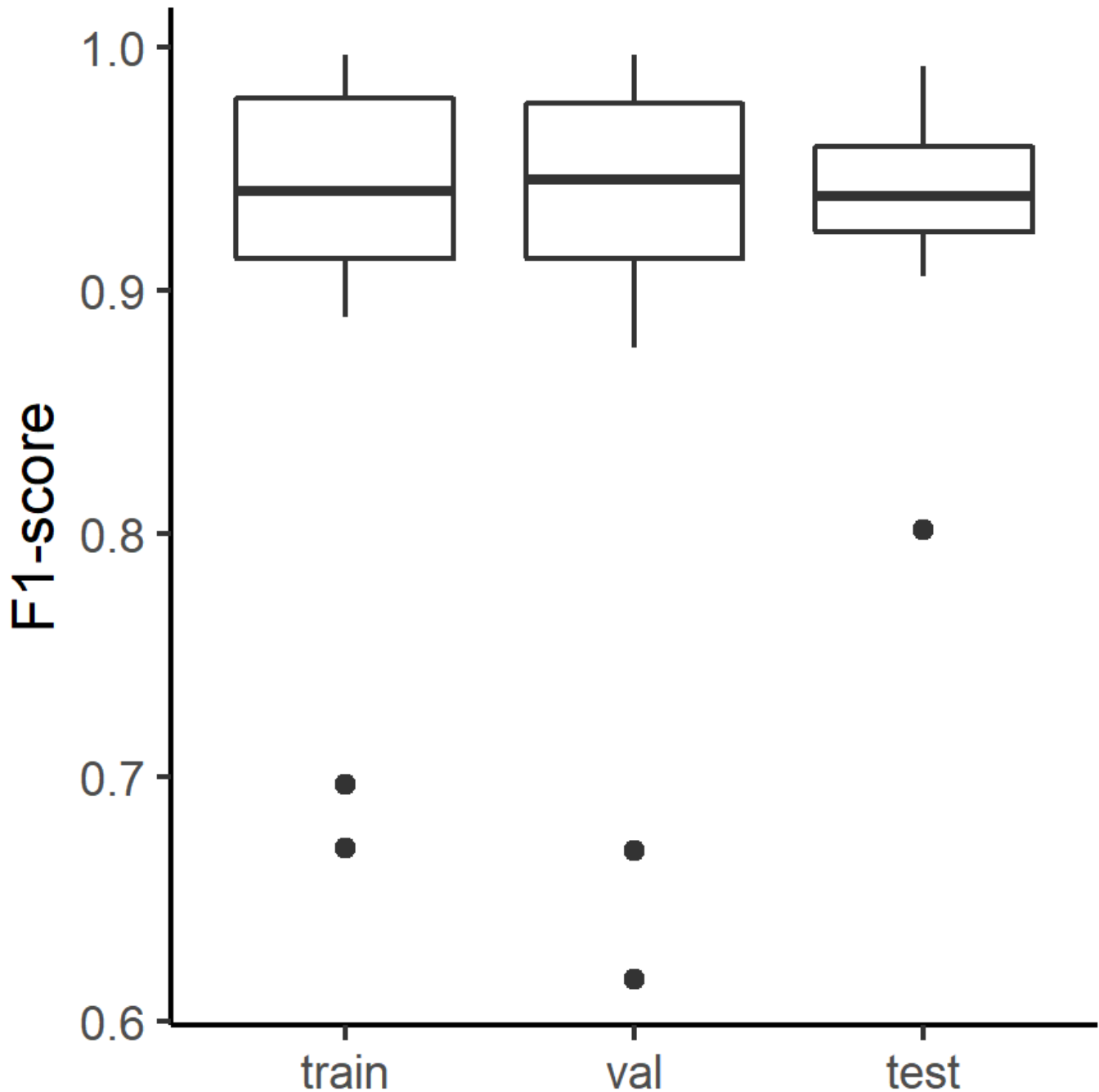


## Figure 3

Prediction results of the final CNN model on the orthoimagery.

Top: The orthoimagery overlaid by the reference polygons (white). Bottom: Orthoimagery overlaid with reference polygons (white) and segmentation results (purple). EPSG: 32735.

